High-β Plasmoid Drift during Pellet Injection into Tokamaks

H. W. Müller, K. Büchl, M. Kaufmann, P. T. Lang, R. S. Lang, A. Lorenz, M. Maraschek, V. Mertens, J. Neuhauser, and ASDEX Upgrade Team

Max-Planck-Institut für Plasmaphysik, EURATOM-IPP Association, Garching, Germany

(Received 21 April 1999)

The outward acceleration of enhanced-β plasmoids formed when a frozen hydrogen pellet is injected into a hot tokamak plasma has been directly observed. The plasmoid characteristics, acceleration, and velocities measured agree with theoretical expectations. The plasmoid motion is always in the positive major radius direction, consistent with high fueling efficiency for high-field side, and rapid mass loss for low-field side injection. In parallel a weak acceleration of the ablating pellet itself in the same direction was observed, probably caused by a net radial rocket force component.

PACS numbers: 28.52.Cx, 52.35.Py, 52.55.Fa

Injection of cryogenic hydrogen isotope pellets still seems to be the most promising option for particle refueling in large toroidal magnetic confinement fusion devices [1]. Future reactor-grade experiments like ITER (International Thermonuclear Experimental Reactor) require densities close to the Greenwald value while retaining a high energy confinement, a requirement which can possibly be met by pellet injection only [2]. Design and optimization of such a system requires sufficient knowledge about the physical mechanisms involved. When a frozen hydrogen isotope pellet is injected into a hot, magnetically confined plasma, pellet material is quickly ablated (in a self-controlled manner), ionized, and heated mostly by fast electron energy influx along magnetic field lines [3]. Since the pellet ablatant mass expansion in the opposite direction is much slower, the energy density in the ablation cloud is rapidly increased over the ambient plasma pressure, and a localized high-β plasmoid is formed [3] ($\beta = 2\mu_0 n k_B T/B^2$; n, T are the plasma density and temperature, k_B the Boltzmann constant, and B the total magnetic field strength).

In practice, the ablation of the frozen pellet along its path across magnetic field lines is not a smooth, continuous process, but is strongly fluctuating ("striations" observed in the emitted light [4]). Various models have been proposed for explanation, e.g., rational magnetic surfaces limiting the locally available energy for ablation, or instability of the ablation process itself, caused by the motion of the frozen pellet relative to its ablation cloud, etc. In effect, this fluctuating ablation is supposed to cause a sequence of more or less separated plasmoids rather than a uniform particle source distribution. According to standard pellet ablation models [4], these plasmoids should attain a cigarlike shape on the μs time scale of primary interest here [5], with a continuously increasing extent along field lines ($\sim$m) and with cross field dimension related to the ionization radius ($\sim$cm) [4].

In the case of an inhomogeneous magnetic field as in toroidal magnetic traps, these diamagnetic high-pressure plasmoids tend to be expelled from the magnetic field [6], with the plasmoid pressure as the driving energy reservoir. The basic physical mechanism is, in a simple picture, vertical charge separation in the plasmoid caused by the toroidally curved magnetic field which drives a radial $\vec{E} \times \vec{B}$ drift of the plasmoid to the magnetic low-field side (LFS) [7,8]. In the case of partial pellet penetration, this drift clearly favors pellet launch from the magnetic high-field side (HFS). This has been experimentally confirmed recently in the ASDEX Upgrade tokamak, where pellet refueling from the HFS turned out to be much more efficient than for conventional low-field side injection [8]. The global drift picture has been reproduced meanwhile also by simulation with a nonlinear 3D resistive plasma code in full toroidal geometry [9], though without a detailed ablation model. On ASDEX Upgrade the study has been significantly extended now, especially by adding a fast multichannel diagnostic, which allows one to investigate the pellet plasmoid dynamics for LFS as well as HFS injection rather in detail. In the present paper we analyze the plasmoid parameters and especially their dynamics and compare them with model predictions.

ASDEX Upgrade is a midsize divertor tokamak (major radius $R_0 = 1.65$ m, plasma radius $a = 0.5$ m, vertical plasma elongation $\kappa = 1.6$, single null divertor). In the experiments described here deuterium (D) pellets were injected via guiding tubes by means of a centrifuge [8], either from the HFS or the LFS (see Fig. 1). The pellet velocity in both cases was 240 ms^{-1}. The pellet repetition rate was varied between 30 and 60 Hz. Because of different pellet sizes the particle content of the pellets was $2.7\text{–}3.8 \times 10^{20}$ atoms.

The experiments described here were performed in D plasmas at a plasma current of $I_P = 800$ kA, a toroidal magnetic field of $B_t = -2.1$ to -1.8 T at the plasma axis, safety factor $q_{95} = 3.9\text{–}4.2$, and a line averaged background plasma density just before pellet injection of $\bar{n}_e = 5.4\text{–}9.4 \times 10^{19}$ m^{-3}. Neutral beam injection of P_{NI} 2.5–5 MW was used for additional plasma heating. The temperatures in the background plasma center were $T_{e0} = 1500\text{–}2200$ eV for the electrons and $T_{i0} = 1500\text{–}2000$ eV

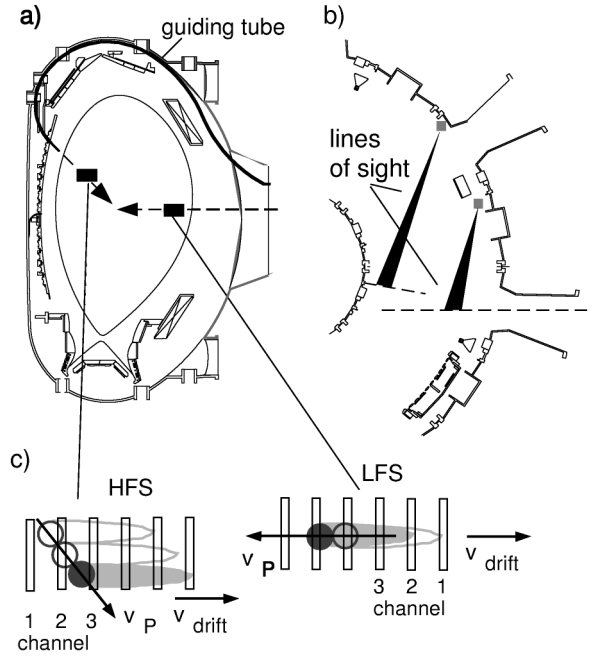

FIG. 1. (a) Poloidal cross section of the ASDEX Upgrade tokamak. Pellets are injected by the centrifuge via guiding tubes. The high-β-drift observation system looks in nearly toroidal direction at the high-β drift. (b) Toroidal cross section of ASDEX Upgrade with pellet injection and observation geometry. (c) Ten lines of sight observe both the HFS and LFS pellet injections (only six are drawn).

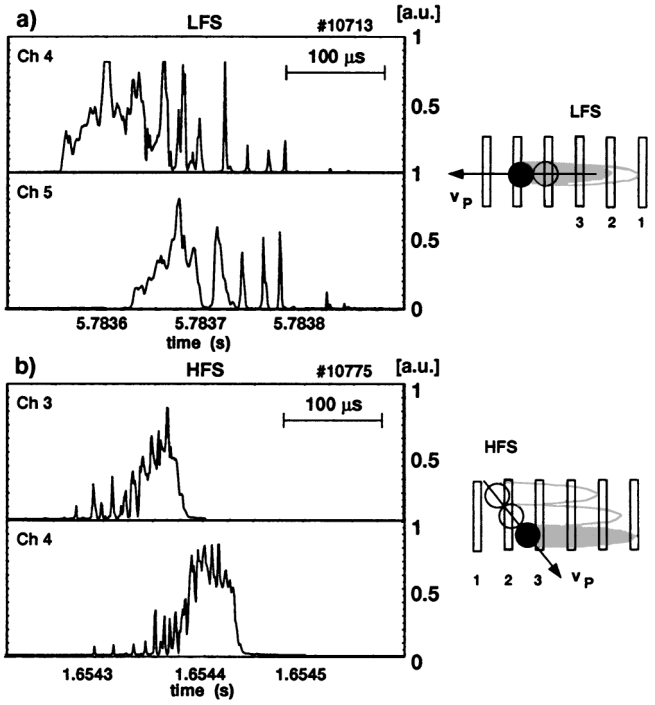

FIG. 2. Time traces of the high-β drift from two neighboring channels of the optical observation system in the case of (a) LFS injection (#10713) and (b) HFS injection (#10775). The signals show continuum emission.

for the ions. The densities were determined by bremsstrahlung measurements calibrated to a DCN laser interferometer. Two fiber arrays were installed inside the tokamak to observe the plasmoid drift, one for the HFS and one for the LFS. Each system has ten lines of sight (channel ch1 . . . ch10) viewing at the pellet path in the toroidal direction. The position of the lines of sight relative to the pellet path can be seen in Figs. 1(b) and 1(c). The radial distance between two neighboring channels is about 15 mm. Each observation channel has a width of 3–4 mm and height of about 30 mm. The light of one line of sight is passing a beam splitting system and detected at two wavelengths with a time resolution of 1 μs. The continuum radiation at 538.1 nm and the D_α line emission were used for the high-β-drift observation. The continuum emission ($\propto n_{e,\mathrm{pl}}^2/\sqrt{T_{e,\mathrm{pl}}}$; $n_{e,\mathrm{pl}}, T_{e,\mathrm{pl}}$ electron density and temperature inside the plasmoid) is especially useful for tracing the dense plasmoids away from the ionization dominated ablation zone. Figure 2 shows the time traces recorded for two neighboring lines of sight for both a LFS and a HFS pellet injection at 538 nm, containing bremsstrahlung and radiation due to recombination.

We first consider two arbitrarily selected channels in a discharge with LFS pellet injection [Fig. 2(a)] ($\bar{n}_e = 5.4 \times 10^{19}$ m^{-3}, $P_{NI} = 2.5$ MW, $T_{e0} \sim 1500$ eV, $T_{i0} = 1500$ eV). The time trace of channel 4 shows a broad emission peak at the beginning followed by several spikes with decreasing intensity. Channel 5, which is closer to the plasma center, has the same signature with a temporal shift of 73 μs corresponding to a velocity of 225 ms^{-1}, slightly below the nominal pellet velocity of 240 ms^{-1}. The spikes following the main peaks are detected up to 200 μs after the onset of the pellet ablation, which is much longer than the time the ablation cloud will need to pass the specific diagnostic channel ($\sim$60 μs). The duration of a spike is down to 1 μs.

In the case of HFS pellet injection the sequence of observations is inverted [Fig. 2(b)] ($\bar{n}_e = 9.4 \times 10^{19}$ m^{-3}, $P_{NI} = 4.9$ MW, $T_{e0} = 1700$ eV). The time traces of both, channel 3 and 4, start with separated spikes of increasing intensity and end with a broad signal. From the end of the broad peaks of the two diagnostic channels a velocity of about 300 ms^{-1} for the major radius component of the pellet motion has been determined. This is much higher than the radial component of the nominal radial pellet velocity of 175 ms^{-1}. We will come back to this point later on.

We emphasize here that the sequence of events for HFS and LFS injection is, in fact, the one expected in the case of a positive major radius plasmoid acceleration to values far above the pellet speed (compare Fig. 2): With injection from the LFS, a specific diagnostic channel will detect radiation emitted from the ablation cloud around the incoming pellet first, resulting in a strong initial signal rise and a relatively broad maximum. After the pellet has crossed

the channel, radiation is still detected, but originating now from plasmoids accelerated backwards, away from the pellet, and arriving at the chosen channel the later, the deeper in they were released from the pellet. Because of expansion and heating of the plasmoids, which both reduce D_α line emission and continuum radiation at 538.1 nm, the intensity of the spikes decreases continuously with increasing time delay relative to the signal onset. In the case of HFS injection plasmoids created near the plasma edge reach a specific line of sight well before the pellet itself crosses the same diagnostic channel. Again those plasmoids created first, traveling a longer distance, have a smaller intensity. Consequently, the signal of a specific HFS channel shows first spikes with gradually increasing amplitude, then reaches a maximum, when the pellet crosses the line of sight and ends abruptly when the pellet together with its shielding cloud has passed.

From the specific HFS pellet launch and diagnostic arrangement, we get further evidence that the drift is in fact in a positive major radius direction, i.e., essentially horizontally outward: The HFS pellets were injected under 44° with respect to the torus midplane while the observation channels are staggered along a horizontal plane (see inlet in Fig. 3). Therefore only some channels of the diagnostic are able to see the pellet with its surrounding ablation cloud. Channels closer to the plasma center will only detect radiation emitted by drifting plasmoids. In Fig. 3 channel 3 shows the typical behavior for HFS injection ($\bar{n}_e = 7.2 \times 10^{19}$ m^{-3}, $P_{NI} = 4.9$ MW, $T_{e0} = 2200$ eV, $T_{i0} = 2000$ eV). As described above, first fluctuations caused by drifting plasmoids can be seen. Later the detected signal ends with a moderately modulated, broad peak, which we attribute to the ablation cloud. In contrast, channels 7 and 8, being closer to the plasma center, show a strongly oscillating signal throughout, with only a vanishing base level in between peaks. Comparing both signals, it is important to note that channels 7 and 8 have higher sensitivity in order to compensate for the decaying emission during the plasmoid drift, and that the largest peaks of channel 7 are in saturation.

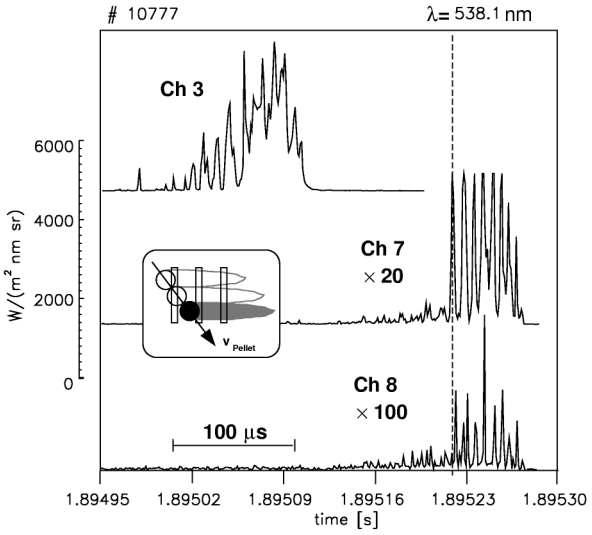

FIG. 3. Signals of high-β-drift diagnostic in the case of HFS pellet injection. Channels 7 and 8 located closer to the plasma center see only drifting plasmoids. The signal of channel 7 is enhanced by a factor of 20, channel 8 by a factor of 100.

From the temperature dependence of the ratio of D_α line emission and continuum radiation, here in the case of not optical thick plasmas, we determined electron temperatures of 2–6 eV for the highly ionized ablation cloud (with an estimated error of about 50%) in agreement with earlier investigations at various tokamaks [4]. Because of the strong density weighting of both the D_α and continuum emission, these values apply mostly to the region of highest plasma density near the pellet. The radiative line emission of the ablation cloud is up to $\sim 10^6$ W/(m^2 sr nm) in the direction of the plasmoid axis. The continuum emission is up to $\sim 10^4$ W/(m^2 sr nm) at 538.1 nm. For several pellets the profile of the D_α line was measured by a spectrometer. The profile is determined by the Lorentz broadening and reabsorption. The typical full width at half maximum is 1.0–2.8 nm, corresponding to densities of 10^{23}–10^{24} m^{-3}, again in agreement with measurements in other tokamaks [4]. These data correspond to substantial plasmoid $\beta_{\rm pl}$ (e.g., $\beta_{\rm pl} = 0.12$ for 3 eV and 2×10^{23} m^{-3}) as compared to typical background plasmas (e.g., $\beta_0 \approx 2 \times 10^{-2}$ for $n_e = 10^{20}$ m^{-3}, $T_e = 1$ keV, and $B = 2T$).

Because of the fluctuating ablation process and possibly further rotational or ballooning-type plasmoid instabilities the emissivity signals obtained can be rather complex as seen above and it is in general not trivial to correlate plasmoid emission peaks. Nevertheless, a peak assignment, sometimes even over five or six channels is possible. A specific HFS injection example is given in Fig. 3. The ablation process itself ends near channel 6 but has obviously produced a few filaments just before, which appear now as a sequence of large peaks on channels 7 and 8. The time delay between these channels of 1–3 μs corresponds to a velocity of 5×10^3 to 1.6×10^4 ms^{-1}. From the peak duration, channel width, and velocity we infer a filament diameter of 1 cm or less.

Analyzing many pellets in a similar way, drift velocities of up to 10^3–10^4 ms^{-1} and average plasmoid acceleration values of 10^8–10^9 ms^{-2} were obtained in good agreement with the theoretically expected acceleration, $a_D = 4\gamma k_B T_{\rm pl}/(mR) \sim 10^9$ ms^{-2} [6] (γ is the adiabaticity coefficient, $T_{\rm pl}$ the plasmoid temperature, m the ion mass, and R the major radius).

Up to this point we have shown that the plasmoids are accelerated over several cm to velocities at least an order of magnitude above conventional pellet velocities. Unfortunately, the rapidly decaying emissivity did not allow one to follow the plasmoids further. There is, however, clear evidence that they can travel a distance of the order of the plasma radius. The most striking one is the rapid

mass loss for LFS injection, which motivated the effort for HFS injection, and the success of the latter. Another more indirect one is that pellets injected from the HFS can trigger neoclassical tearing mode activity in the central plasma, a fact which has not been observed for LFS injection.

Altogether, both LFS and HFS experiments indicate that, in hot plasmas, ablation plasmoids can travel over distances comparable to the order of the minor plasma radius. This may be understood in terms of a simple MHD model consideration. We assume a local high pressure perturbation to be created in a tokamak background plasma on a μs time scale by parallel electron heat transport. As mentioned earlier, such a plasmoid is initially not in local force balance and is therefore accelerated in a major radius direction towards a new equilibrium with a strongly perturbed magnetic field. The time needed to establish the corresponding perturbed equilibrium current is of the order of the Alfvén transit time over a connection length, $\tau \sim \pi q R/v_A \sim 5$ μs (v_A is shear Alfvén velocity), which is much faster than the plasmoid expansion along field lines with about sound speed. Together with the radial acceleration a_D discussed above, this results in a typical radial displacement $s \sim \Delta\beta_{\mathrm{av}}\gamma\pi^2 q^2 R$, essentially proportional to the connection length averaged plasmoid beta enhancement $\Delta\beta_{\mathrm{av}}$, consistent with 3D resistive MHD simulations [9]. In practice $\Delta\beta_{\mathrm{av}}$ is a fraction of the local plasmoid beta, since the plasmoid expansion has at this time reached a fraction of the connection length only.

As shown above, the pellet velocity derived from the diagnostic array signals shows a clear deviation from the nominal one. The velocity of the pellets injected from the HFS has not been directly measured, but the time of flight through funnel and guiding tube yields a typical mean velocity for this distance of about 230 ± 35 ms^{-1}. This means that the pellet velocity was nearly unchanged in the guiding system compared to the nominal pellet speed at the centrifuge of 240 ms^{-1}, in accordance with earlier laboratory measurements [10]. The horizontal component of the HFS injected pellet velocity is therefore only $\sim$175 ms^{-1}. In consequence, the pellet is obviously accelerated along its path inside the plasma. Velocities of up to $\sim$350 ms^{-1} (about twice the nominal speed) in the horizontal direction were measured. On average, an acceleration of the order $4-7 \times 10^5$ ms^{-2} is estimated.

In support, an average pellet velocity beyond the nominal one is independently calculated from the pellet penetration depth taken from video pictures together with the duration of pellet ablation determined from the D_α emission pulse length.

In the case of LFS pellet injection the pellet velocity inside the plasma is typically found to be less than the nominal pellet velocity. The observation starts here close to the plasma edge, where a mean velocity of $230-240$ ms^{-1} was found. During the ablation the pellet is decelerated on its inward path with $\sim -4 \times 10^5$ ms^{-2}. The acceleration of the pellet is in both cases, LFS and HFS pellet injection, directed towards the magnetic LFS, i.e., in the same direction as the ablation plasmoids, though several orders of magnitude smaller.

A possible explanation is a small net rocket force component in radial direction, caused by a poloidally asymmetric pellet mass ablation and momentum transfer. This in-out asymmetry could be directly caused by the impact of a fraction of the drifting cloud ionized at the HFS of the pellet, or indirectly, by a HFS-LFS variation of the parallel heat flux shielding.

In conclusion, the outward acceleration of enhanced-β plasmoids formed when a hydrogen pellet is injected into a hot tokamak plasma has been directly observed. The maximum radial plasmoid velocities observed were up to 2 orders of magnitude above the pellet velocity. Triggering of core MHD activity for HFS injection and rapid mass loss for LFS injection in hot plasmas indicate a displacement comparable to the minor plasma radius, in accordance with theory. An acceleration of the solid pellet in the same direction has been observed, probably caused by a net radial rocket force component. The fact that the plasmoid motion is always to the LFS explains the success of HFS pellet injection.

[1] M. Greenwald *et al.*, Nucl. Fusion **28**, 2199 (1988).
[2] D. J. Campbell *et al.*, Fusion Energy 1998, Proceedings of the 17th International Conference, Yokohama, IAEA-F1-CN-69/ITER/1-ITERP1/01 (IAEA, Vienna, to be published).
[3] M. Kaufmann, K. Lackner, L. Lengyel, and W. Schneider, Nucl. Fusion **27**, 171 (1986).
[4] S. L. Milora, W. A. Houlberg, L. L. Lengyel, and V. Mertens, Nucl. Fusion **35**, 657 (1995).
[5] R. D. Durst, Ph.D. thesis, University of Texas, 1988.
[6] L. L. Lengyel, Nucl. Fusion **17**, 805 (1977).
[7] V. Rozhansky, I. Veselova, and S. Voskoboynikov, Plasma Phys. Controlled Fusion **37**, 399 (1995).
[8] P. T. Lang *et al.*, Phys. Rev. Lett. **79**, 1487 (1997).
[9] H. R. Strauss and W. Park, Phys. Plasmas **5**, 2676 (1998).
[10] K. Büchl and W. Sandmann, Max-Planck-Institut für Plasmaphysik, Garching, IPP Report, 5/83, 1998.